RESEARCH ARTICLE

INTERNATIONAL MICROBIOLOGY (2013) 16:235-242
doi: 10.2436/20.1501.01.199 ISSN 1139-6709 **www.im.microbios.org**

INTERNATIONAL MICROBIOLOGY
OPEN ACCESS

Bacterial adhesion efficiency on implant abutments: A comparative study

Marina Etxeberria,[1,2] Lidia López-Jiménez,[1] Alexandra Merlos,[1] Tomás Escuín,[2] Miguel Viñas[1]*

[1]Laboratory of Molecular Microbiology and Antimicrobials. Department of Pathology and Experimental Therapeutics, University of Barcelona, Barcelona, Spain. [2]Laboratory of Prosthodontics, Department of Dentistry, Medical and Dentistry Schools, University of Barcelona, IDIBELL, Barcelona, Spain

Received 28 October 2013 · Accepted 5 December 2013

Summary. The attachment of *Escherichia coli* ATCC 25922 and *Staphylococcus aureus* ATCC 28213 onto six different materials used to manufacture dental implant abutments was quantitatively determined after 2 and 24 h of contact between the materials and the bacterial cultures. The materials were topographically characterized and their wettability determined, with both parameters subsequently related to bacterial adhesion. Atomic force microscopy, interferometry, and contact angle measurement were used to characterize the materials' surfaces. The results showed that neither roughness nor nano-roughness greatly influenced bacterial attachment whereas wettability strongly correlated with adhesion. After 2 h the degree of *E. coli* attachment markedly differed depending on the material whereas similar differences were not observed for *S. aureus*, which yielded consistently higher counts of adhered cells. Nevertheless, after 24 h the adhesion of the two species to the different test materials no longer significantly differed, although on all surfaces the numbers of finally adhered *E. coli* were higher than those of *S. aureus*. [**Int Microbiol** 2013; 16(4):235-242]

Keywords: implant abutments · glass fiber · bacterial adhesion · nano-roughness · wettability · biomaterials

Introduction

Bacteria can grow as sessile forms (biofilms) on almost all surfaces and under almost any environmental condition. In most infectious diseases, particularly those arising from infected implants and medical devices, bacterial growth as biofilms plays a crucial role in disease pathogenesis [6]. Among all known biofilms occurring in pathologic settings, those in the oral cavity provide a good model system and as such have been extensively studied [13]. Oral biofilms are formed by a wide variety of gram-positive and gram-negative bacteria species and are a consistent feature of oral infections, mainly caries, periodontitis, and endodontitis, but they are also involved in infection-related implant failures, so-called peri-implantitis [23]. The adhesion and development of microbial biofilms depend upon the characteristics of the microbes that form them, but also on the environmental conditions. Chemical and surface properties such as roughness, nano-roughness, and wettability are relevant in controlling bacterial adhesion [28].

*Corresponding author: M. Viñas
Laboratory de Microbiologia Molecular
Facultat de Medicina. Universitat de Barcelona
Feixa Llarga s/n
08907 Hospitalet de Llobregat, Spain
Tel. +34-934024265
E-mail: mvinyas@ub.edu

One of the main goals of oral implantology is to significantly reduce the risk of infection, e.g., by altering the local environment such that it is less favorable for bacterial biofilm formation. Accordingly, the elucidation of the mechanisms underlying bacterial adhesion, colonization, and biofilm development on prosthetic devices and implant surfaces is currently an area of great interest in both clinical and biomedical research. From a biomechanical engineering standpoint, the physical properties of implant surfaces can be optimized by taking advantage of recent progress in both materials science and nanotechnology. By modulating cell-substrate interactions, for example, the biological response of the infectious agent can be determined [2,23,27].

The effect of surface topography on cell attachment has received significant attention, with several recently published studies highlighting the critical role in cellular adherence played by nanotopography [19,20,22]. Nano-engineered surfaces can directly influence bacterial behavior, as shown in studies demonstrating that these cells align in the anisotropic direction of microscale ridges and grooves [14]. Based on these findings, a possible approach to restrict biofilm formation involves the use of materials whose surface properties hinder biofilm development, particularly in the early stages of implantation [13]. Different strategies can be adopted to achieve this purpose, such as by altering the nanoscale surface topography. However, there is no consensus regarding whether increased surface roughness correlates either positively or negatively with the extent of bacterial attachment. Clearly, materials enhancing biofilm formation should be discarded even if they have excellent mechanical properties.

Metals, ceramics, polymers, and composites are currently used to manufacture prosthetic implant abutments. Among these materials, glass fiber-reinforced composites (glass-FRC) are a promising low-cost alternative to metal alloys, metal ceramics, and ceramic restorations. Indeed, in the last few years glass-FRCs have been used successfully in a variety of dental applications [1,10]. Implant-supported fixed prostheses of glass-FRC may also offer a suitable alternative [5,11], but the potential and limitations of this promising material have not been adequately evaluated.

A few studies have specifically examined the effect of the nanoscale morphology of dental implant abutment materials, and especially titanium, on surface-bacteria interactions in vitro. However, little is known about the extent of bacterial attachment on nanometrically characterized implant abutment surfaces, whether of titanium or other metals. Experimental approaches to explore topography with respect to bacterial adhesion include experimental bacteriology, atomic force microscopy (AFM), interferometry, and wettability measurements. In this study, we analyzed and compared the surface properties, roughness, and wettability of six test materials used in the manufacture of implant abutments in terms of the adhesion of the gram-positive bacterium *Staphylococcus aureus* and the gram-negative bacterium *Escherichia coli*. Our aim was to evaluate the biocompatibility of glass-FRC and the potential application of this material in dentistry.

Materials and methods

Dental materials. Disks 10 mm in diameter and 2 mm thick were manufactured from each of six different implant abutment materials. The tested materials were: (i) Cast cobalt-chromium disks obtained from acrylic resin patterns (Pattern Resin LS, GC Corp.) and invested with phosphate-bonded investment material (CM-20 Cendrex+Métaux, Biel/Bienne, Switzerland) as indicated by the manufacturer (BEGO, Bremer Goldschlägerei Wilh. Herbst, Bremen, Germany). Casting was accomplished using Co-Cr Wirobond C alloy (BEGO). After melting and casting by induction (Ducatron Série 3 UGIN'Dentaire, Seyssins, France), the disks were sandblasted with 110-µm aluminum oxide particles (Korox, BEGO) under 3 bar pressure to remove oxide films and residual investment. (ii) Selective laser melted (SLM) Co-Cr disks (BEGO). Both the cast and the SLM Co-Cr disks were polished in three stages: (a) using a hard rubber disk at 15,000 rpm; (b) then with a soft rubber disk at 15,000 rpm, and (c) using a soft brush with a polishing paste at 1400 rpm. Each polishing phase lasted 90 s. (iii) Machined and polished titanium grade V disks (Klockner-Soadco, Andorra). (iv) Zirconia (Y-TZP) disks (Dentisel, Barcelona, Spain). (v) Glass-FRC disks, prepared from rods (Bioloren, Saronno, Varese, Italy). And (vi) polyetheretherketone (PEEK) disks, prepared from rods (Teknimplant, Barcelona, Spain). All disks were handled by their lateral walls. They were gently cleaned using a cotton pellet with ethanol and dried under warm dry air.

Surface characterization. The disk surfaces were analyzed by three different methods: (i) Atomic force microscopy. It was carried out with an AFM XE-70 (Park Systems, Korea) in non-contact mode. The rectangular-shaped cantilever (ACTA Si-cantilevers, Park Systems) had a force constant of 40 N/m, a resonance frequency of 300 kHz, and a tip radius with a curvature of <10 nm. All AFM variables, including scan rate and set point, were optimized for the type of sample measured. Scan areas were 5 × 5 µm², with a scan rate of 0.6 Hz and a resolution of 256 × 256 pixels. AFM images were processed using a scanning probe image processor XEI (Park Systems), correcting the plane of the AFM image for possible coupling of the lateral plane and the *z*-axis, caused by the instrument. The height, area, and volume of the surfaces were determined via polygon/ellipse/circle methods, in which a suitable shape is best fitted to the image. The average surface roughness (Ra) was calculated. (ii) White light interferometry; the specimens were visualized on a white light interferometer microscope (LeicaSCAN DCM3D, Leica Microsystems, Switzerland), which is a computerized optical interference microscope operating in the vertical scanning interferometry mode and producing a topographic image. The objective used was Leica N Plan H 50×/0.50, with an Mirau-interferometer objective lens and an image resolution of 250.64 × 190.90 µm². Images were analyzed using the software Leica map DCM 3D 6.2.6561 version (Leica Microsystems); the threshold was set to 1.0% and the Gauss filter to 25 µm. Ra was determined. And (iii) surface wettability measurements; they were conducted by measuring the contact angle using the sessile water-drop method [13,24]. Briefly, 10 µl of MilliQ-quality water was dropped onto the center of each specimen using an injector. Digital photo-

Table 1. Bacterial adhesion expressed as colony-forming units (CFU)/mm² (average of 16 determinations). SLM, selective laser melted; PEEK polyetheretherketone

	Staphylococcus aureus		*Escherichia coli*	
Material	CFU/mm² (2 h)	CFU/mm² (24 h)	CFU/mm² (2 h)	CFU/mm² (24 h)
Cast Co-Cr	1.82×10^2	7.74×10^4	6.38×10^1	4.46×10^6
SLM Co-Cr	1.14×10^2	6.38×10^4	4.56	4.92×10^6
Titanium	1.18×10^2	6.83×10^4	1.41×10^1	7.84×10^6
Zirconia	3.42×10^2	3.37×10^5	1.00×10^1	4.92×10^6
GF-reinforced composite	2.64×10^2	4.15×10^5	2.73×10^2	4.24×10^6
PEEK	1.00×10^2	5.92×10^4	2.51×10^2	5.65×10^6

graphs were taken (Nikon D70) and the resulting images were analyzed using IMAT software (CCIT, Barcelona, Spain). Sixteen samples were measured in each group, with each disk measured twice.

Bacterial strains and culture media. Two collection bacterial strains were used to assess the adhesion properties of gram-negative and gram-positive bacteria on the test materials: *Escherichia coli* strain ATCC 25922 and *Staphylococcus aureus* strain ATCC 28213, respectively. Both strains were maintained on trypticase soy agar (TSA, Sharlau, Barcelona, Spain) plates. Adhesion experiments were carried out using two colonies selected from the plates to inoculate trypticase soy broth (TSB, Scharlau). The cultures were incubated at 37 ºC in a rotary shaker at 240 rpm in air for 18 h, at which time they had reached the late exponential phase of growth.

Adhesion experiments. Disks to be used in the bacterial assays were sterilized in an autoclave (121 ºC, 15 min). The above-described overnight cultures were diluted in TSB to the desired concentration (10^6 colony forming units [CFU]/ml in TSB), as determined spectrophotometrically. For the adhesion experiment, the disks were covered with a suspension of the bacterial culture and incubated at 37 ºC with gentle (60 rpm.) shaking. samples were taken 2 and 24 h later, processing the disks by washing them four times in Ringer's 1/4 to remove unattached bacteria and then placing them in test tubes containing 1 ml of Ringer's 1/4. The tubes were submerged in an ultrasonic water bath for 3 min, vigorously vortexed for 1 min, and then treated ultrasonically again for 3 min to release the surface-attached bacteria. Serial dilutions (10^0 to 10^{-7}) of these suspensions were used to inoculate agar plates, which were incubated for 48 h. Colonies were then scored and counted. The detachment of biofilm-forming bacteria from the disks was monitored by microscopic visualization of the disks after sonication and vortexing.

Atomic force microscopy imaging. Bacteria were cultured in liquid media in which disks of tested materials were submerged; disks were then washed four-fold by using Ringer's 1/4 and allowed to dry on air. Samples were imaged in air by using an atomic force microscope XE-70 [Park Systems]. All images were collected in non-contact mode by using rectangular-shaped silicon cantilevers with a spring constant of ± 40 N/m and a resonance frequency of ±300 kHz. The upper surface of these cantilevers (the opposite side of the tip) is coated with aluminium to enhance the laser beam reflectivity. The data acquired during the surface scanning were converted into images of topography, amplitude and phase; and analysed by using XEP and XEI software (Park Systems). On topography images, it becomes possible to observe the shape, structure and differences of the sample surface, amplitude images accentuating the edges gives roughness and height information. Finally, the phase images show variations in elasticity and viscoelasticity of the sample. The four types of image were simultaneously acquired with scan size of 25 μm² at a scan rate of 0.6 Hz.

Table 2. Roughness values as determined by interferometry and atomic force miscroscopy. SLM, selective laser melted; PEEK, polyetheretherketone

	Roughness	Nanoroughness
	White light interferometry	Atomic force interferometry
Material	Ra (μm)	Ra (nm)
Cast Co-Cr	0.0776	48
SLM Co-Cr	0.0388	14
Titanium	0.0474	29
Zirconia	0.108	136
GF-reinforced composite	0.553	236
PEEK	0.113	59

Results

Bacterial adhesion of gram-positive *S. aureus* and gram-negative *E. coli* onto disks of the tested materials were compared. The results are summarized in Table 1. Surface roughness, determined as the mean arithmetic surface roughness (Ra), was characterized by interferometry and AFM, as shown in Table 2. The angles formed between water and the test materials resulted to be as follows: the lowest angle (75º 64′) was formed on zirconia, followed by cast Co-Cr (79º 71′); three of the tested materials gave quite similar angles: SLM Co-Cr (85º 4′), Titanium (84º 23′) and PEEK (89º 75′), whereas the highest value corresponded to GF-reinforced composite (113º 36′). A set of selected images showing the surface roughness are presented for comparison in Fig. 1 (interferometry) and Fig. 2 (AFM).

Imaging of bacterial cells grown as sessile forms onto the different tested material surfaces allowed to distinguish details concerning adhesion and morphologies. Fig. 3 shows two AFM images of both *E. coli* and *S. aureus* when developing biofilms onto glass-FRC.

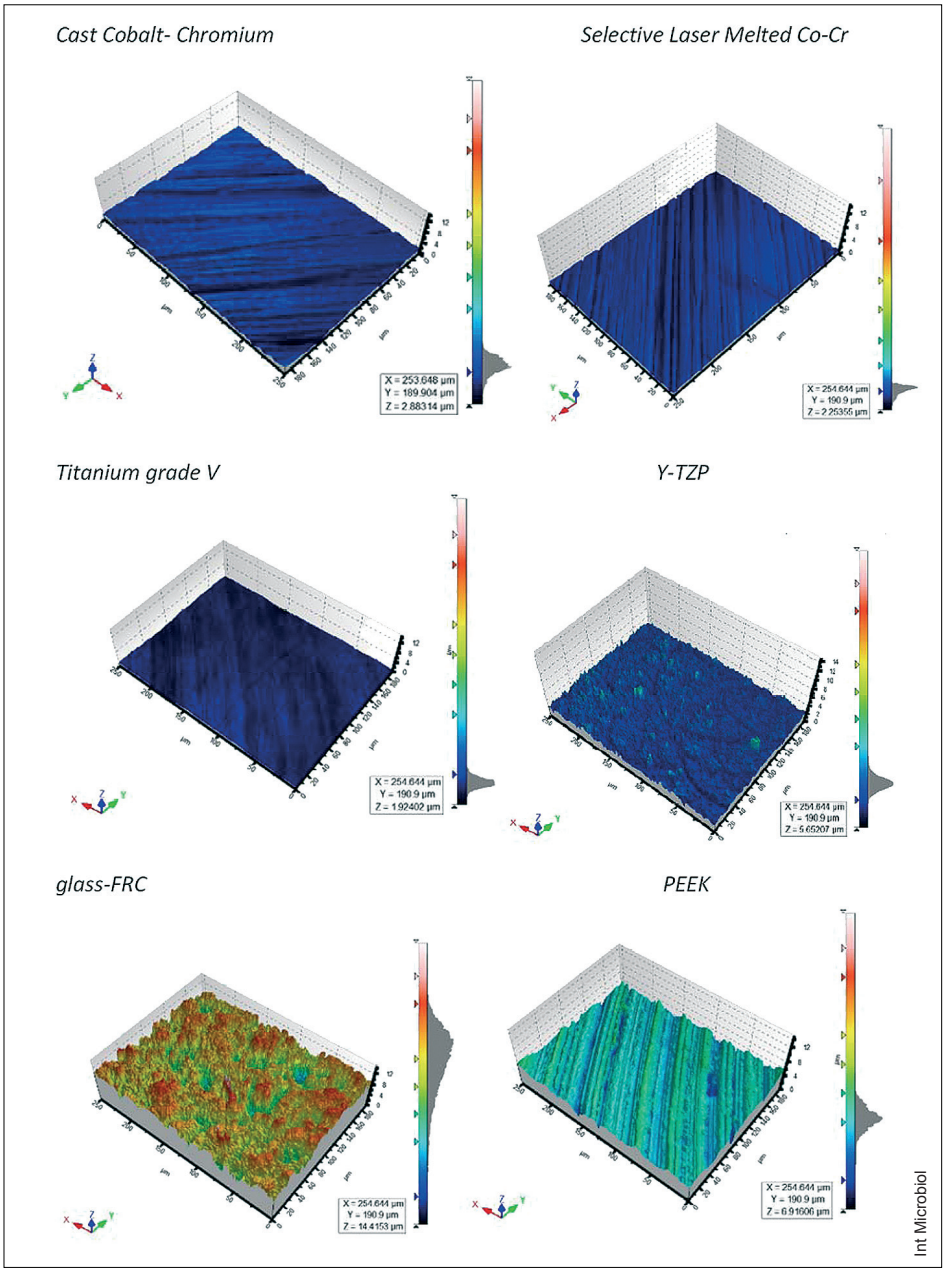

Fig. 1. Interferometry images of the six surface materials tested. (**A**) Cast cobalt- chromium. (**B**) Selective laser melted cobalt-chromium. (**C**) Titanium. (**D**) Zirconia (Y-TZP). (**E**) Glass-FRC. (**F**) PEEK polyetheretherketone.

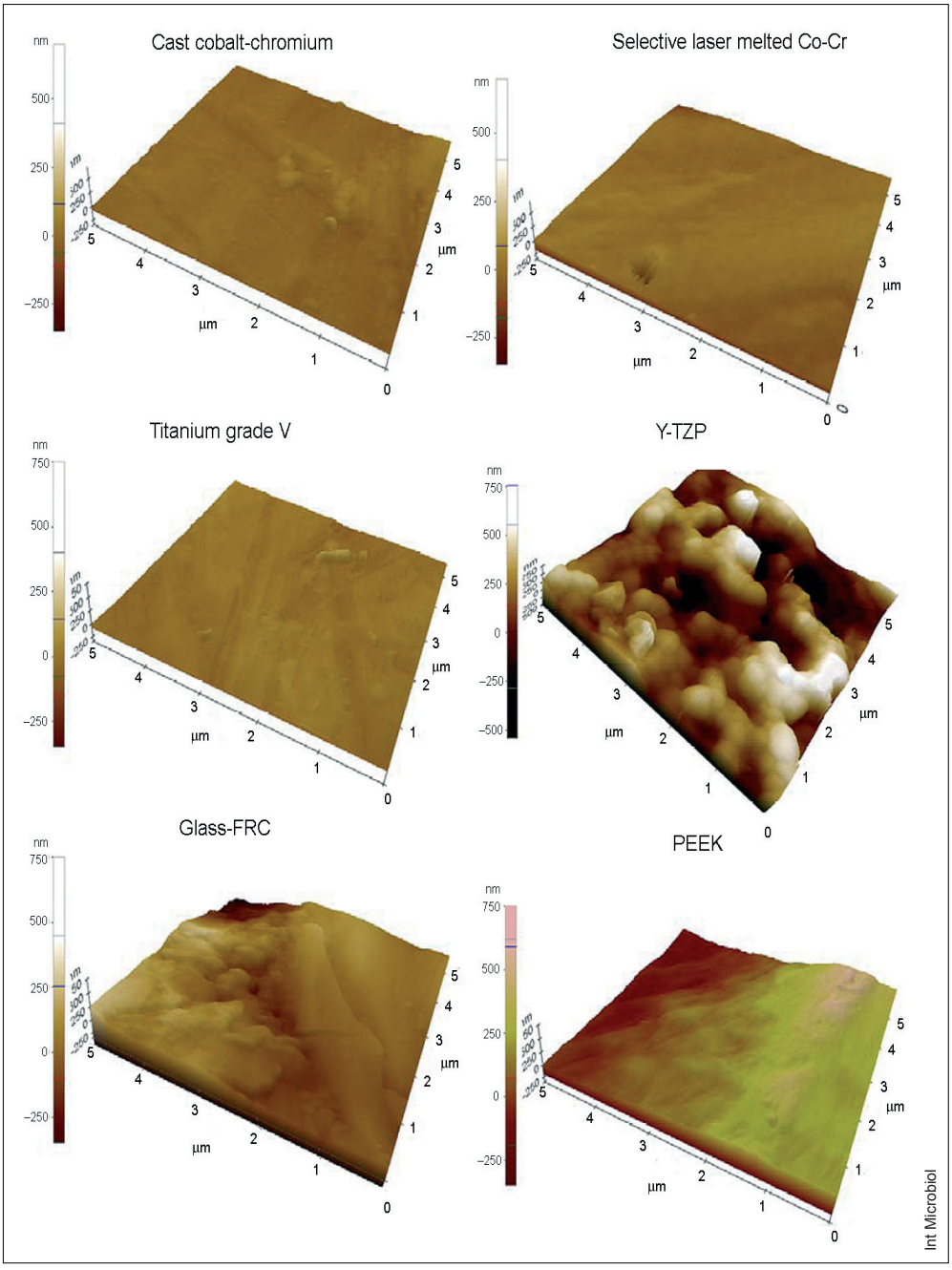

Fig. 2. AFM imaging of the six surface materials tested. (**A**) Cast cobalt-chromium. (**B**) Selective laser melted cobalt-chromium. (**C**) Titanium. (**D**) Zirconia (Y-TZP). (**E**) Glass-FRC. (**F**) PEEK polyetheretherketone.

Discussion

The ability of bacteria to form biofilms is among the most relevant factors in the pathogenesis of peri-implantitis and periodontitis. Since both gram-positive and gram-negative bacteria cause oral infections, in this study representatives of each one (*E. coli* and *S. aureus*) were used to determine bacterial adhesion to the six tested materials. Our primary aim was to compare the efficiency of bacterial adhesion onto implant abutments currently in use, especially glass-FRC in order to assess its potential advantages. This focus reflects current interest in glass-FRC as an alternative to traditionally used materials. A recent report, showed that the use of glass-FRC for implant abutment or restoration material could significantly reduce physical stresses in the bone-implant contact area by

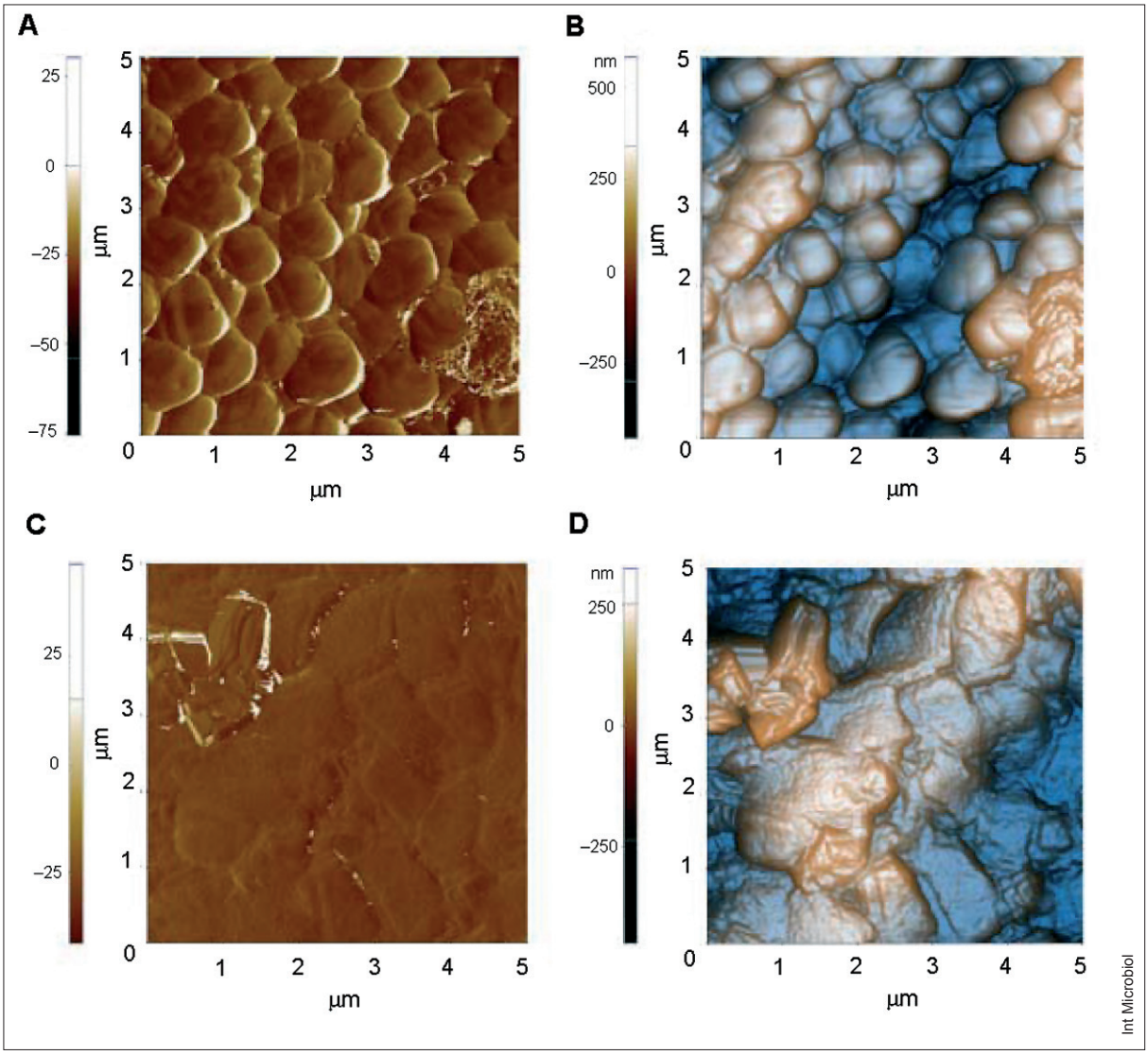

Fig. 3. AFM imaging on glass-FRC disks: (**A**) *Staphylococcus aureus* phase; (**B**) *S. aureus* topography; (**C**) *Escherichia coli* phase; (**D**) *E. coli* topography.

acting as shock-absorbers and thus minimize the risk of eventual peri-implant bone loss [18]. However, there is still much to be learned about the potential application of glass-FRC. Progress in nanotechnology allows the design and production of materials, including biomaterials, with surface properties tailored to a given application. Today, one of the main focuses of biomaterials research is the physico-chemical properties of surfaces that determine bacterial adhesion [25].

In this study, the surface parameters of dental materials were measured using three different methodologies. In surface roughness analyses, we found important differences between the studied materials, with glass-FRC being significantly rougher than the other biomaterials examined, both at micro- and nano-scales. Interferometry measurements of surface roughness showed higher values for glass-FRC than for either zirconia (5-fold) or titanium (10-fold). Similar results were obtained with AFM, which showed that the nano-roughness of glass-FRC was twice that of zirconia and eight times that of titanium. Nonetheless, the high Ra value of glass-FRC falls within the clinically acceptable range [4,25] (Table 2). The most highly polished surface was that of SLM chrome cobalt, followed by titanium. This result contradicts a previous report in which significantly greater differences in the Ra values of similar materials, including laser sinterized chrome cobalt, were reported, although in that study a profilometer was used whereas our measurements were obtained with AFM [16].

Likewise, zirconia was much rougher when assessed using AFM rather than interferometry. The discrepancy could be due to the well-recognized differences in roughness depending on the measurement method used and to the fact that zirconia surfaces are strongly affected by the material preparation procedure. In a recent study, glazing procedures were shown to reduce the surface roughness of Y-TZP [20]. In our study, AFM imaging demonstrated strong surface differences between zirconia and cast Co- Cr, laser sinterized Co-Cr, and titanium (Fig. 2).

There have been a few reports examining the relationship between nanoscale topographical details and bacterial adhesion. Microbial adhesion was shown to be sensitive to nanoscale topography (commonly accepted with feature sizes <100 nm) but universal rules of attachment have yet to be determined. For example, some investigators have observed that the attachment of certain bacteria is higher on surfaces with nanophase than with conventional topographies [15,20], while others have found a bacteria-repelling effect of nanophase materials [19]. Our results, like those of do Nascimento et al. [7,8], do not provide insights into the relationship between roughness and bacterial adhesion.

In bacterial attachment, contact between the cell and the surface is maximized. This process is aided by the ability of bacteria to assume different morphologies and to alter the number and size of their appendages, such as flagella or pili, or the amount of capsular material depending on the topographical details of the target surface or the physiological state or growth phase [14]. Gains in our knowledge of adhesion properties have important implications for the bioengineering of materials not only for use in the oral cavity but also with respect to a wide range of medical devices.

Wettability is another key determinant of bacterial adhesion efficiency. In our study, the degree of surface hydrophobicity positively correlated with the degree of surface roughness, with the roughest surface exhibiting the highest surface hydrophobicity. This correlation is in accordance with the Wenzel model, which explains roughness-induced hydrophobicity [27], and with a 2011 study reporting similar roughness-wettability correlations [15].

Our conclusions regarding bacterial adhesion are based on experiments with two different bacterial species, *S. aureus* and *E. coli*, as mechanisms of adhesion are strongly dependent upon the structure of the bacterial envelope and thus reflect the two major types of biological and chemical organization of the bacterial surface. Although our results cannot be mechanistically extended to all microbes, large differences with other oral pathogens are not expected. As seen from the data in Table 1, the dependence of adhesion on the physicochemical properties of the test materials was already evident after 2 h of incubation, since the most polished surface adsorbed the lowest amount of bacteria and vice-versa. After 24 h, differences in bacterial adhesion to the test surfaces were no longer significant, consistent with the findings in previous reports [3, 9]. While at 2 h *S. aureus* adhered more efficiently, by 24 h *E. coli* adhesion had increased.

Bacterial growth on glass-FRC was similar to that measured on titanium, confirming the results obtained in a previous study [17].The absence of a difference between the different surfaces may have been due to their wettability, since glass-FRC, is less wettable than the other materials tested. More research is needed assessing these aspects and other possible factors that may have influenced the results.

Acknowledgements.We thank Teresa Tomas for her excellent technical assistance in the preparation of the dental materials. This work was partially supported by "Ajuts a la Recerca" awarded to the School of Dentistry, University of Barcelona. The generous gift of abutment materials from Bego (Bremen, Germany), Klockner-Soadco (Andorra), Dentisel (Barcelona, Spain), Bioloren (Varese, Italy) and Tekniimplant (Barcelona, Spain) is gratefully acknowledged.

Competing interests. None declared

References

1. Adbulmajeed A, Walboomers X F, Massera J, Kokkari A K, Vallittu P K, Närhi TO (2013) Blood and fibroblast responses to thermoset BisGMA-TEGDMA/glass fiber-reinforced composite implants *in vitro*. Clin Oral Implants Res first published online: 16 apr 2013.doi: 10.1111/clr.12151
2. Anselme K, Davidson P, Popa AM, Giazzon M, Liley M, Ploux L (2010) The interaction of cells and bacteria with surfaces structured at the nanometre scale. Acta Biomater 6:3824-3846
3. Almaguer-Flores A, Olivares-Navarrete R, Wieland M, Ximénez-Fyvie LA, Schwartz Z, Boyan BD (2012) Influence of topography and hydrophilicity on initial oral biofilm formation on microstructured titanium surfaces *in vitro*. Clin Oral Implants Res 23:301-307
4. Barbosa SH, Zanata RL, Navarro MFL, Nunes OB (2005) Effect of different finishing and polishing techniques on the surface roughness of microfilled, hybrid and packable composite resins. Braz Dent J 16:39-44
5. Behr M, Rosentritt M, Lang R, Handel G. (2001) Glass fiber-reinforced abutments for dental implants. A pilot study. Clin Oral Implants Res 12:174-178
6. Costerton W, Veeh R, Shirtliff M, Pasmore M, Post, C. Ehrlich, G. (2003) The application of biofilm science to the study and control of chronic bacterial infections. J Clin Invest. 112:1466-1477
7. do Nascimento C, da Rocha Aguiar C, Pita MS, Pedrazzi V, de Albuquerque RF Jr, Ribeiro RF (2013) Oral biofilm formation on the titanium and zirconia substrates. Microsc Res Tech 76:126-132
8. do Nascimento C, Pita MS, Fernandes FHNC, Pedrazzi V, de Albuquerque RF Jr, Ribeiro RF (2013) Bacterial adhesion on the titanium and zirconia abutment surfaces. Clin Oral Implants Res 00:1-7; first published online:doi: 10.1111/clr.12093

9. Egawa M, Miura T, Kato T, Saito A, Yoshinari M (2013) In vitro adherence of periodontopathic bacteria to zirconia and titanium surfaces. Dent Mater J 32:101-106
10. Fischer H, Weber M, Eck M, Erdrich A, Marx R (2004) Finite element and experimental analyses of polymer-based dental bridges reinforced by ceramic bars. J Biomech 37:289-294
11. Freilich MA, Meiers JC, Duncan JP, Eckrote KA, Goldberg AJ (2002) Clinical evaluation of fiber-reinforced fixed bridges. J Am Dent Assoc 133:1524-1534
12. Gittens RA, Olivares-Navarrete R, Cheng A, et al. (2013) The roles of titanium surface micro/nanotopography and wettability on the differential response of human osteoblast lineage cells. Acta Biomater 9:6268-6277
13. Gorth DJ, Puckett S, Ercan B, Webster TJ, Rahaman M, Bal BS (2012) Decreased bacteria activity on $Si_3 N_4$ surfaces compared with PEEK or titanium. Int J Nanomedicine 7:4829-4840
14. Hsu L, Fang J, Borca-Tasciuc DA, Worobo RW, Moraru CI (2013) The effect of micro- and nanoscale topography on the adhesion of bacterial cells to solid surfaces. Appl Environ Microbiol 79:2703-2712
15. Ivanova EP, Truong VK, Webb HK, Baulin VA, Wang JY, Mohammodi N, Wang F, Fluke C, Crawford RJ (2011) Differential attraction and repulsion of *Staphylococcus aureus* and *Pseudomonas aeruginosa* on molecularly smooth titanium films. Sci Rep 1:165-177
16. Kilicarslan MA, Ozkan P (2012) Evaluation of retention of cemented laser-sintered crowns on unmodified straight narrow implant abutments. Int J Oral Maxillofac Implants 28:381-387
17. Lassila LV, Garoushi S, Tanner J, Vallittu PK, Söderling E (2009) Adherence of *Streptococcus mutans* to fiber-reinforced filling composite and conventional restorative materials. Open Dent J 4:227-232
18. Magne P, Silva M, Oderich E, Boff LL, Enciso R. (2013) Damping behavior of implant-supported restorations. Clin Oral Implants Res 24:143-148
19. Puckett S D, Taylor E, Raimondo T, Webster TJ (2010) The relationship between the nanostructure of titanium surfaces and bacterial attachment. Biomaterials 31:706-713
20. Rizzello L, Sorce B, Sabella S, Vecchio G, Galeone A, Brunetti V, Cingolani R, Pompa PP (2011) Impact of nanoscale topography on genomics and proteomics of adherent bacteria. ACS Nano 5:1865-1876
21. Sabrah AH, Cook NB, Luangruangrong P, Hara AT, Bottino MC (2013) Full-contour Y-TZP ceramic surface roughness effect on synthetic hydroxyapatite wear. Dent Mater 29:666-673
22. Singh AV, Patil R, Thombre DK, Gade WN (2013) Micro-nanopatterning as tool to study the role of physicochemical properties on cell-surface interactions. J Biomed Mater Res A 101:3019-3032
23. Subramani K, Jung RE, Molenberg A. Hämmerle CH (2009) Biofilm on dental implants: a review of the literature. Int J Oral Maxillofac Implants 24:616-626
24. Truong VK, Lapovok R, Estrin YS, Rundell S, Wang JY, Fluke CJ, Crawford RJ, Ivanova EP (2010) The influence of nano-scale surface roughness on bacterial adhesion to ultrafine-grained titanium. Biomaterials 31:3674-3683
25. Uçtaşli MB, Bala O, Güllü A (2004) Surface roughness of flowable and packable composite resin materials after finishing with abrasive discs. J Oral Rehabil.31:1197-1202
26. Variola F, Brunski J, Orsini G, Tambasco de Oliveiran P, Wazen R, Nanci, A. (2011) Nanoscale surface modifications of medically-relevant metals:state-of-the art and perspectives. Nanoscale 3:335-3532
27. Wenzel RN (1949) Surface roughness and contact angle. J Phys Colloid Chem 53:1466-1467
28. Zareidoost A, Yousefpour M, Ghaseme B, Amanzadeh A (2012) The relationship of surface roughness and cell response of chemical surface modification of titanium. J Mater Sci Mater Med 23:1479-1488